

Seasonal temperature responses to land-use change in the western United States

Lara M. Kueppers^{a,*}, Mark A. Snyder^{a,*}, Lisa C. Sloan^a, Dan Cayan^{b,c}, Jiming Jin^d,
Hideki Kanamaru^b, Masao Kanamitsu^b, Norman L. Miller^d,
Mary Tyree^b, Hui Du^e, Bryan Weare^e

^a Department of Earth and Planetary Sciences, University of California, Santa Cruz, 1156 High Street, Santa Cruz, CA 95064, USA

^b Scripps Institution of Oceanography, University of California, San Diego, 8605 La Jolla Shores Drive, La Jolla, CA 92093, USA

^c United States Geological Survey, University of California, San Diego, 8605 La Jolla Shores Drive, La Jolla, CA 92093, USA

^d Earth Sciences Division, Lawrence Berkeley National Laboratory, 1 Cyclotron Road, Mail-stop 90-1116, Berkeley, CA 94720, USA

^e Department of Land, Air and Water Resources, University of California, Davis, 1 Shields Ave., Davis, CA 95616, USA

Received 26 April 2006; received in revised form 12 February 2007; accepted 9 March 2007

Available online 30 March 2007

Abstract

In the western United States, more than 79 000 km² has been converted to irrigated agriculture and urban areas. These changes have the potential to alter surface temperature by modifying the energy budget at the land–atmosphere interface. This study reports the seasonally varying temperature responses of four regional climate models (RCMs) – RSM, RegCM3, MM5-CLM3, and DRCM – to conversion of potential natural vegetation to modern land-cover and land-use over a 1-year period. Three of the RCMs supplemented soil moisture, producing large decreases in the August mean (–1.4 to –3.1 °C) and maximum (–2.9 to –6.1 °C) 2-m air temperatures where natural vegetation was converted to irrigated agriculture. Conversion to irrigated agriculture also resulted in large increases in relative humidity (9% to 36% absolute change). Modeled changes in the August minimum 2-m air temperature were not as pronounced or consistent across the models. Converting natural vegetation to urban land-cover produced less pronounced temperature effects in all models, with the magnitude of the effect dependent upon the preexisting vegetation type and urban parameterizations. Overall, the RCM results indicate that the temperature impacts of land-use change are most pronounced during the summer months, when surface heating is strongest and differences in surface soil moisture between irrigated land and natural vegetation are largest.

© 2007 Elsevier B.V. All rights reserved.

Keywords: irrigated agriculture; land-use change; regional climate model (RCM); surface radiation budget; urban land-cover

1. Introduction

Anthropogenic land-cover and land-use changes have dramatically altered the earth's surface, with agriculture, pasture, and urban land occupying more than 54 million km² (Leff et al., 2004), or 41% of Earth's ice-free land area. These large-scale changes affect fresh water quality and quantity, biodiversity, carbon cycling,

* Corresponding authors. Tel.: +1 831 459 3504; fax: +1 831 459 3074.

E-mail addresses: lkueppers@ucmerced.edu (L.M. Kueppers), msnyder@es.ucsc.edu (M.A. Snyder).

¹ Present address: School of Natural Sciences, University of California, Merced, P.O. Box 2039, Merced, CA 95344, USA.

and climate (Sala et al., 2000; Watson et al., 2000; Pielke et al., 2002; Feddema et al., 2005). Agricultural expansion and land management practices have both direct and indirect consequences for regional meteorology and climate. Use of mineral fertilizers and extensive tilling can result in soil carbon losses (Lal and Bruce, 1999), while more sustainable management can help soil sequester atmospheric carbon dioxide (Watson et al., 2000). Conversion of natural ecosystems to farmland alters the surface roughness of vegetation, albedo, leaf conductance, and other properties that affect exchanges of water and energy between the land surface and atmosphere (Pielke et al., 2002). Irrigation may also have a significant atmospheric impact. In global modeling studies, irrigation results in decreased surface temperatures, increased relative humidity, and changes in the temperature profile of the troposphere, with geographic variations in the strength of these effects (Boucher et al., 2004; Lobell et al., 2006).

Urban development also has consequences for local and regional meteorology. Urban climatic processes such as turbulent atmospheric fluxes and the urban heat island have been extensively documented (Arnfeld, 2003). Replacing natural vegetation with roads and buildings often decreases the surface albedo and alters the local surface energy balance, increasing sensible heat flux and decreasing latent heat flux. Measurements have detected differences in intra-urban air temperatures as large as 9 °C (Eliasson and Svensson, 2003) and 12 °C (Oke, 1981). Previous modeling work at smaller spatial scales has suggested that even modest shifts in urban albedo and soil moisture levels can cause large changes in energy partitioning, local temperature, and winds (Sailor, 1995; Jacobson, 1999). In the United States, impervious surface area covers over 100 000 km² (Elvidge et al., 2004), with the potential to affect water percolation, runoff, evaporation, and radiation balance. Although they cover relatively large areas, and have measurable influence on the local atmosphere, urban land-cover types and characteristics are often not included in climate modeling studies.

2. The semi-arid western United States

The coterminous western United States U.S. (Fig. 1) has seen rapid and extensive changes in land-use over the past 150 years, and urban/suburban growth is projected to continue at a rate three times faster than the rest of the U.S., for at least the next 50 years (Population Reference Bureau, 2004). This region is primarily semi-arid, with summer drought in many sub-regions. Irrigation has been used to overcome rainfall deficiencies on

over 73 000 km² (USDA, 2004). Irrigation has resulted in unnaturally high evapotranspiration fluxes from many agricultural areas, with implications for local and regional water and energy budgets, and possibly atmospheric dynamics. Large cities have replaced a variety of natural vegetation types on more than 6000 km² in this region, with implications for temperature, humidity, and air quality. The western U.S. also has high topographic variability, including several mountain ranges that are not captured by general circulation model (GCM) boundary conditions. Representation of realistic topography in such regions is extremely important for robust climate prediction (Giorgi et al., 1997; Snyder et al., 2002). To quantify the effects of past urban and agricultural land-use change, and to incorporate the influence of the region's variable topography, this study used a regional climate modeling approach.

Regional climate models (RCMs) are used to investigate climate processes within limited domains, taking in large-scale climate information from GCMs or global observational datasets at their lateral boundaries. A number of RCMs have been previously validated and used for the western United States (e.g., Chen et al., 1999; Anderson et al., 2000; Kim, 2001; Kim et al., 2002; Bell et al., 2004; Leung et al., 2004; Snyder and Sloan, 2005), and improve the representation of climate relative to GCMs. This study used an RCM intercomparison approach to determine the modeled temperature sensitivity to conversion of natural vegetation to agricultural and urban land-uses. By comparing results from several RCMs, it is possible to identify common temperature responses to land-cover and land-use change in the western U.S.

3. Materials and methods

3.1. Experimental design

This study used four RCMs (RSM, RegCM3, MM5-CLM3, and DRCM, described in detail in Section 3.3) to conduct a set of climate model sensitivity experiments to determine a range of seasonal temperature responses to the introduction of irrigated agriculture and urban land. Each model was run for two cases in which the land surface characteristics were changed, while all other initial and boundary conditions were held constant. Multiple boundary conditions and irrigation parameterizations were used across the models in order to identify common responses under a variety of model configurations (Table 1). The first run (MOD) used a modern vegetation distribution that included both irrigated and non-irrigated agriculture, as well as urban

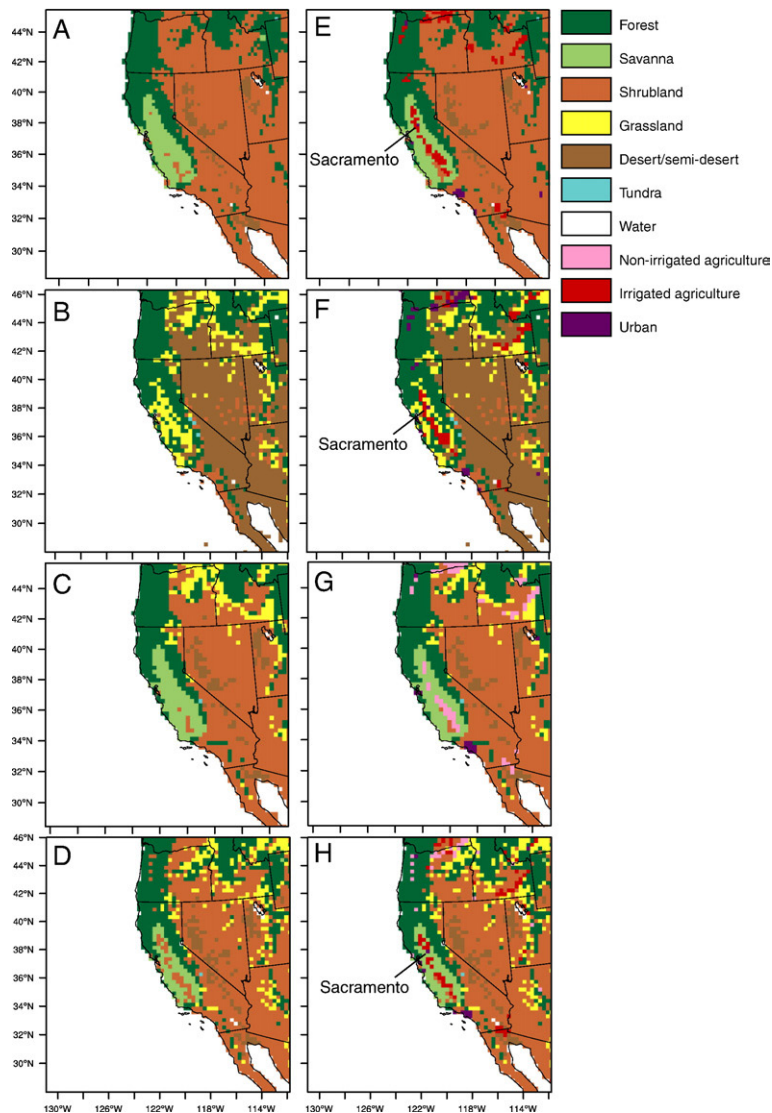


Fig. 1. Potential natural (NAT) and modern (MOD) land cover types as represented by the four models. Types are aggregated into broader categories in this plot: (A) NAT case RSM; (B) NAT case RegCM3; (C) NAT case MM5-CLM3; (D) NAT case DRCM; (E) MOD case RSM; (F) MOD case RegCM3; (G) MOD case MM5-CLM3; (H) MOD case DRCM.

land. The second run (NAT) used potential natural vegetation distribution designed for this experiment (see Section 3.2). The land surface data for the NAT runs do not include any agricultural or urban land-cover types.

3.2. Land-cover datasets and parameterizations

In climate models, the land surface is represented with a limited suite of land-cover and vegetation types. Associated parameters describe the albedo and roughness height of the canopy, and depending on the model, physiological properties such as leaf conductance and monthly variation in leaf area. The modern land-cover

descriptions for RSM, RegCM3, and MM5-CLM3 were derived from the Global Land Cover Characteristics (GLCC) database (version 2.0), which in turn is based on 1-km Advanced Very High Resolution Radiometer (AVHRR) data collected from April 1992 to March 1993 (Loveland et al., 2000). The potential natural land-cover description was created at 1-km resolution based on the GLCC data by replacing anthropogenic types with their nearest-neighbor natural vegetation types. The resulting vegetation distributions were checked for consistency with the Ramankutty and Foley (1999) potential natural vegetation dataset. Because each RCM utilized a slightly different suite of natural and anthropogenic

Table 1
Parameters and parameterizations for irrigated agriculture and urban land represented in the four RCMs

	Irrigated agriculture parameters				Urban parameters			
	RSM	RegCM3	MM5-CLM3	DRCM	RSM	RegCM3	MM5-CLM3	DRCM
Maximum vegetation cover (%)	90	80	85	80	95	5	0	10
Roughness length (m)	0.06	0.06	0.06	0.07	0.2287	1.5	0.01	0.5
Displacement height (m)	N/A	0.0	0.34	N/A	N/A	6.0	N/A	N/A
Minimum stomatal resistance (s/m)	40	45	N/A	36	999	120	N/A	999
Maximum leaf area index	N/A	6	6	4	N/A	1	N/A	4
Top soil layer depth (cm)	10	10	1.75	7	10	10	1.75	7
Total soil depth (m)	2	3	3.4	2.55	2	3	3.4	2.55
Soil texture type (sand/silt/clay, %)	Sandy loam (58:32:10) ^a	Loam (43:39:18)	Sandy clay loam (58:15:27) ^a	Multiple	Loamy sand (82:12:6) ^a	Clay (22:20:58)	Sand (92:5:3) ^a	Multiple
Vegetation albedo ^b	VIS: 0.10 NIR: 0.30	VIS: 0.08 NIR: 0.28	VIS: 0.11 NIR: 0.58	Total: 0.15–0.19	VIS: 0.09 NIR: 0.29	VIS: 0.02 NIR: 0.15	N/A	Total: 0.15
Soil moisture modification	Saturation (all time steps)	Field capacity (all time steps)	None	$4.8225 \times 10^{-8} \text{ m s}^{-1 \text{ c}}$	None	None	None	Fixed at 0.05 kg/kg

^a Soil types are parameterized separately from vegetation types; values given are the dominant values for the urban and agricultural grid cells in the MOD case.

^b VIS is for the visible range (0.4–0.7 nm); NIR is for the near-infrared range (>0.7 nm).

^c $4.8225 \times 10^{-8} \text{ m s}^{-1}$ when the top soil layer temperature is greater than 12 °C, and zero when less than 12 °C.

land-cover types, custom translations of the Olsen Global Ecosystems version of the GLCC data were created for each model. Both MOD and NAT land-cover datasets were aggregated separately for each model to the coarser resolution (25–30 km) grids used in the experiments (Fig. 1). In the DRCM regional climate model, an earlier version of the GLCC database (Love-land et al., 1995) was used to specify MOD vegetation. For the NAT case in DRCM, all urban and agricultural land in MOD was replaced with the “shrubland” vegetation type. The resulting land-cover distributions differed in the exact number and types of vegetation categories among the models (Fig. 1).

Irrigation timing and amount vary geographically at much finer spatial scales than a typical RCM grid cell size. In addition, water rights are held tightly in the western U.S., so spatially explicit data on irrigation is scarce. The four models varied in the manner by which soil moisture was altered to mimic irrigation in the irrigated cropland land-cover type, ranging from saturation at all time steps to no modification of soil moisture (Table 1). The models also differed in prescribed soil properties, canopy properties, and vegetation cover for agricultural types (Table 1). Finally, RegCM3, MM5-CLM3, and DRCM represented monthly changes in crop properties, such as leaf area, whereas RSM did not.

Like irrigation, variation in the properties of urban land occurs at resolutions finer than the RCM grids. However, the footprint of urban areas is significant

enough to warrant inclusion in land surface models (Jin et al., 2005). The urban land-cover type was parameterized differently among the models (Table 1). In DRCM the soil moisture was fixed at a low level at all time steps but was not explicitly modified in the other three models. None of the models included the effects of anthropogenic heat release due to combustion (Sailor, 1995).

3.3. Model descriptions

3.3.1. RSM

The version of the Regional Spectral Model (RSM) (Juang and Kanamitsu, 1994) used for this study was originally developed at the National Centers for Environmental Prediction (NCEP), and was subsequently updated at the Experimental Climate Prediction Center (ECPC) of the Scripps Institution of Oceanography (SIO) (Kanamitsu et al., 2005). The RSM applies sine and cosine series to the deviation of the full forecast field from the global base field (perturbations), and is capable of very accurate and efficient spectral calculations (Juang and Kanamitsu, 1994). A “scale selective bias correction scheme” (Kanamitsu and Kanamitsu, 2005) was used to reduce error relative to the reanalysis boundary conditions in the large-scale (>1000 km) fields within the regional domain. RSM uses the relaxed Arakawa–Schubert convection scheme (Moorthi and Suarez, 1992) and the radiation package of Chou (Chou and Suarez, 1994; Chou and Lee, 1996). The land

surface model is the Oregon State University Land Scheme (OSU2, Pan and Mahrt, 1987), which includes 12 vegetation types and 2 soil layers.

3.3.2. RegCM3

The International Center for Theoretical Physics (ICTP) Regional Climate Model, RegCM3 (Pal et al., in press), is a third-generation regional-scale climate model derived from the National Center for Atmospheric Research–Pennsylvania State (NCAR–PSU) MM5 mesoscale model. RegCM3 includes the same dynamical core as MM5. RegCM3 includes the Biosphere–Atmosphere Transfer Scheme (BATS1E) (Dickinson et al., 1993) for surface process representation and the CCM3 radiative transfer package (Kiehl et al., 1996). RegCM3 documentation and source code are available at www.ictp.trieste.it/RegCNET/model.html. For these experiments, RegCM3 was configured with the Grell cumulus scheme (Grell, 1993) utilizing the Fritsch and Chappell closure scheme (Fritsch and Chappell, 1980) and the Holtslag boundary layer scheme (Holtslag and Boville, 1993). This version of BATS has 22 land-cover types and 3 soil layers, with rooting depth and other soil properties linked to land-cover type (Table 1).

3.3.3. MM5-CLM3

The non-hydrostatic version of the NCAR/Penn State (PSU) Mesoscale Model version 5.v3.6 (MM5) coupled with the NCAR Community Land Model version 3 (CLM3) was used here (Jin and Miller, submitted for publication-a). This study used the Grell convection scheme (Grell, 1993), and the Medium Range Forecast (MRF) planetary boundary layer (PBL) scheme (Hong and Pan, 1996). The radiation scheme was taken from Community Climate Model version 2 (CCM2) (Kiehl et al., 1994). Mass and heat transfer are described using a simple crop scheme. In this version, a sophisticated surface albedo scheme was adopted to improve the surface energy balance simulations (Oleson et al., 2004; Jin and Miller, submitted for publication-a). Introduction of a maximum of 8 sub-cells within each CLM3 cell improves the accuracy of the land surface characterization and the land surface–atmosphere water and energy flux exchanges. Cropland in CLM3 is specified according to leaf area index, roughness height, and vegetation fraction. This version of CLM3 has 24 land-cover types and 10 soil layers.

3.3.4. DRCM

The Davis Regional Climate Model (DRCM) is derived from the NCAR–PSU MM5V3.6 mesoscale model (Chen and Dudhia, 2001). The configuration

used in this study includes the five-phase (cloud drops, rain, ice, snow, and graupel) Goddard precipitation scheme (Lin et al., 1983; Tao et al., 1989), the relaxed Arakawa–Schubert convection (Grell, 1993), the Mellor–Yamada 2.5-level planetary boundary layer scheme (Janjic, 1990, 1994), the Rapid Radiation Transfer Model (Mlawer et al., 1997), and a slightly modified version of the fully interactive Noah land surface model vegetative surface/hydrology scheme (Chen and Dudhia, 2001). The physical attributes of the vegetation for summer and winter are specified for 24 land-cover types. The soil is represented with 4 layers, and soil properties were defined for 19 soil types.

All four RCMs used a common domain centered on 37.5°N/121.5°W, spanning approximately 29°N to 45.5°N and 110°W to 132°W (100°W to 140°W for DRCM). RSM was run at a 25 km horizontal resolution, and RegCM3, MM5-CLM3, and DRCM at 30 km. RSM, RegCM3, and MM5-CLM3 used the NCEP/DOE Reanalysis II (Kanamitsu et al., 2002) as lateral boundary condition data, while DRCM used the ECMWF Reanalysis (ERA-40) (Gibson et al., 1997). All models were run from 1 October 1995 through 30 September 1996, a year with average precipitation. RegCM3 runs started in October 1993, MM5-CLM3 runs started in September 1995, and DRCM runs started in August 1995 to allow additional time for model spin-up. All models used prescribed sea surface temperatures (SSTs) over the ocean from the National Oceanic and Atmospheric Administration Optimally Interpolated Sea Surface Temperature (NOAA OISST) dataset (Reynolds et al., 2002) for the appropriate time period. Finally, the models used similar CO₂ concentrations, held constant for the two experimental runs (348 ppm in RSM, 355 ppm in RegCM3 and MM5-CLM3, and 330 ppm in DRCM).

As a model validation step, this study compared monthly average output from the MOD runs by the four RCMs to gridded observations from the University of East Anglia Climate Research Unit (CRU) high-resolution, time-series dataset TS2.1 (Mitchell and Jones, 2005), including 2 m mean, maximum, and minimum temperatures, temperature range, precipitation and surface vapor pressure. This report focuses on January and August 1996, as they represent the wet/cool and dry/warm seasons, respectively, in this region.

4. Results

4.1. Modern RCM results compared with observations

All four models captured regional variations in August 2 m mean air temperature (T_{mean}) except in

California's Central Valley, where RSM, RegCM3 and DRCM showed a cool bias (Fig. 2). RSM and RegCM3 also underestimated T_{\max} in parts of the Central Valley by up to ~ 8 °C, where soil moisture was supplemented under irrigated cropland (not shown). The cool biases in irrigated regions in the three models supplementing soil moisture, with less bias in MM5-CLM3, suggest that soil moisture is prescribed to be too high where irrigation is specified, or the resolution of the models (and perhaps the CRU data) is too coarse to capture spatial variation in land-use. DRCM underestimated August T_{\max} by ~ 4 – 8 °C throughout the modeled domain (not shown). The models also captured the broad patterns in January T_{mean} , with cool biases in DRCM and MM5-CLM3 in parts of Nevada and a warm bias in RSM in Central California (Fig. 2). Some of the models had modest to substantial cold biases of ~ 4 °C in January T_{\max} in individual subregions, but only DRCM underestimated T_{\max} over most of the region (not shown). All of the models overestimated observed January T_{\min} by up to ~ 5 °C along the central California coast and in the Central Valley (not shown). RSM, RegCM3, and DRCM also overestimated T_{\min} in Nevada and eastern Oregon (not shown). As a result of warm biases in T_{\min} and cool biases in T_{\max} , all four models underestimated the diurnal temperature range (DTR) by up to ~ 10 °C throughout the model domain in January, and RSM and DRCM underestimated DTR in August by ~ 8 °C (not shown). CRU DTR varies from 12 °C to more than 24 °C in August, and from 5 °C to more than 15 °C in January in this region. The consistent underestimation across models and seasons could be due to differences in how DTRs are calculated between the models and data, or to actual dampened diurnal cycles in the models.

All of the models produced more spatial variability in August precipitation than is evident in the CRU observations in this summer-dry region (not shown). All models overestimated January precipitation in the high precipitation areas of northern coastal California, the Oregon Cascade Range, and the Sierra Nevada range when compared to CRU observations (Fig. 3). However, given the scarcity of weather stations in these remote areas, and the interpolation approach used to create the CRU dataset, the true discrepancy between models and interpolated data is poorly constrained. Finally, RSM overestimated August and January vapor pressure by ~ 4 – 12 hPa in areas specified as irrigated agriculture, particularly in California's Central Valley and Imperial Valley, where CRU vapor pressure is ~ 8 – 20 hPa (not shown), likely a result of prescribing saturated soil in these areas. DRCM underestimated surface vapor pressure in much of California and western Arizona,

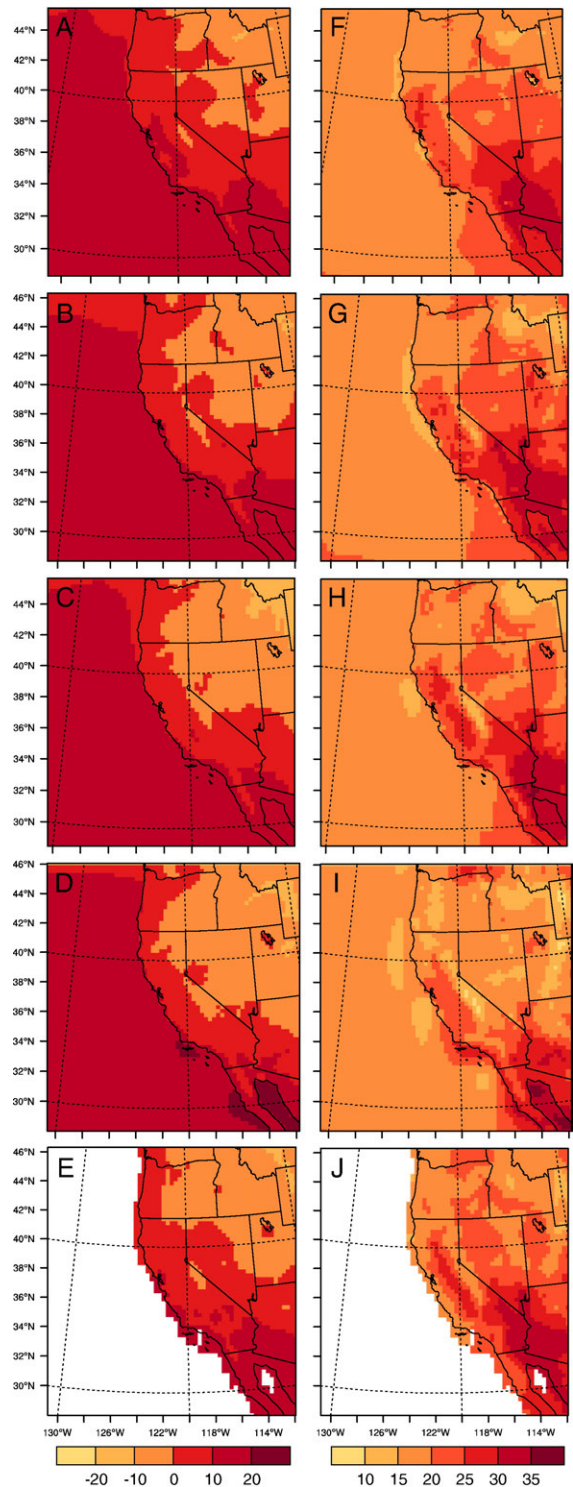


Fig. 2. January (left column) and August (right column) mean 2-m temperature (°C) from the four MOD cases and CRU observations: (A) January RSM; (B) January RegCM3; (C) January MM5-CLM3; (D) January DRCM; (E) January CRU; (F) August RSM; (G) August RegCM3; (H) August MM5-CLM3; (I) August DRCM; (J) August CRU.

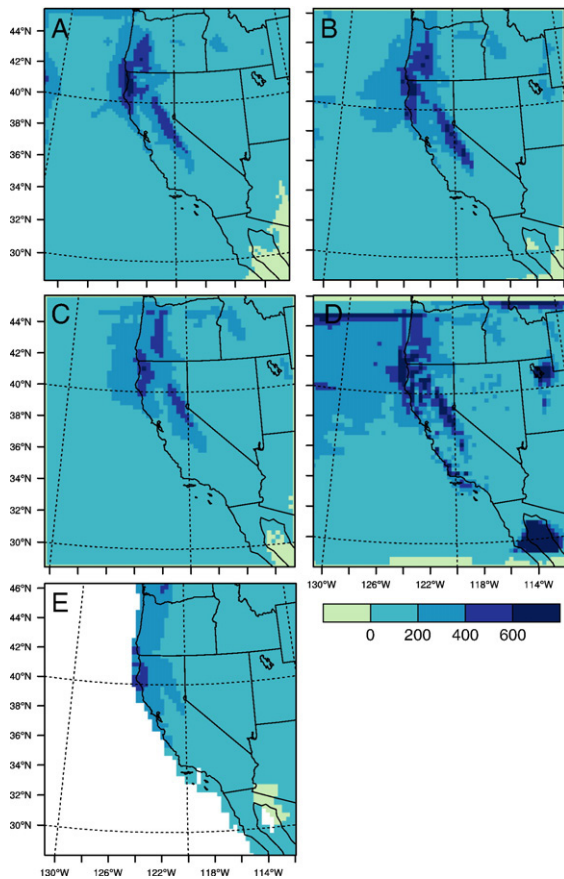


Fig. 3. January precipitation (mm) from the four MOD cases and CRU observations: (A) RSM; (B) RegCM3; (C) MM5-CLM3; (D) DRCM; (E) CRU.

while RegCM3 underestimated vapor pressure in southeastern California in January (not shown).

4.2. Effects of converting natural vegetation to irrigated agriculture

The temperature effects of converting potential natural vegetation to irrigated agriculture were quantified as the difference between the two cases, MOD – NAT, for each model and all variables. Temperature responses were qualitatively consistent across models, and varied strongly through the seasons. While DRCM applied a temperature criterion to determine irrigation timing, both RSM and RegCM3 supplemented soil moisture at every time step throughout the year, and MM5-CLM3 did not include irrigation. Nonetheless, across the three models that included irrigation, the resulting differences in soil moisture in irrigated areas between the cases were minimal between December and

February, and most pronounced from June to September due to seasonal variation in precipitation and solar radiation, particularly in California's Central Valley (Fig. 4). The seasonal variation in T_{\max} , T_{mean} , and latent heat flux differences follows the soil moisture pattern, with more muted variation (and diverging model responses to irrigation) for T_{\min} (Fig. 4). MM5-CLM3, which did not supplement soil moisture, produced very little change throughout the year for the same variables, reinforcing the relatively large influence of soil moisture, and proportionally small influence of other canopy properties in irrigated agricultural areas, on temperature.

To determine the spatial extent and spatial variability in modeled temperature responses, we examined January (wet season) and August (dry season) means. In August, RSM, RegCM3, and DRCM all produced widespread temperature differences: T_{mean} and T_{\max} were reduced several degrees (-1.4 to -6.1 °C), averaged over all areas converted to irrigated agriculture (Table 2), with the largest decreases occurring in the Central and Imperial Valleys in RegCM3 (Fig. 5). By way of comparison, the interannual range in August mean temperature spans 3.9 °C over the 102 years of the CRU TS2.1 dataset, averaged over the same irrigated areas. August T_{\min} responses were less consistent among the models, with T_{\min} rising in RSM, declining in RegCM3, and with no discernible effect in DRCM (Table 2). As a result of the above changes, RSM, RegCM3, and DRCM produced substantial decreases in DTR in irrigated areas (Table 2).

The August temperature changes reflected large modifications to the water and energy budgets during this warm, dry part of the year. Top layer soil moisture in RSM, RegCM3, and DRCM was increased substantially with irrigation (Fig. 6 and Table 2). This led to ~fivefold increases in latent heat flux in these three models (Fig. 7 and Table 2). Sensible heat flux decreased by 76–100 W/m² (Table 2), a change opposite in sign but similar in magnitude to the change in latent heat flux. Net long-wave flux also decreased slightly in both RSM and RegCM3. RSM and RegCM3 both produced strong increases in relative humidity in irrigated areas, with a more pronounced effect in RSM (36%) than in RegCM3 (23%) (Table 2). DRCM produced a smaller increase in relative humidity (9%).

Averaged over all irrigated areas, January temperature changes were modest across the models (Fig. 5 and Table 2). The small January temperature changes reflect the minor differences in soil moisture, and consequent energy fluxes, between the two cases during the rainy season (not shown). Unlike the other models,

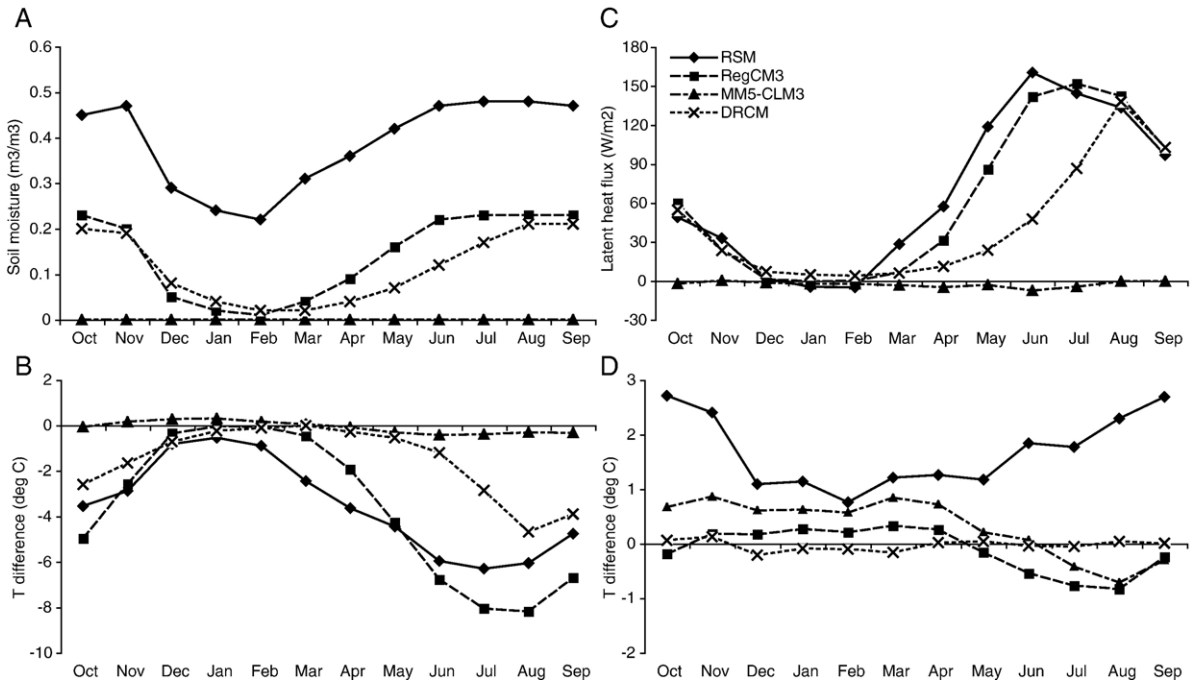


Fig. 4. Monthly variation in climate differences between MOD and NAT cases averaged over irrigated agriculture in the Central Valley for the four models ($n=44$ for RSM, $n=27$ for RegCM3, $n=21$ for MM5-CLM3, and $n=21$ for DRCM). (A) Monthly soil moisture anomalies (m^3/m^3); (B) monthly maximum 2-m temperature anomalies ($^{\circ}\text{C}$); (C) monthly latent heat flux anomalies (W/m^2); (D) monthly minimum 2-m temperature anomalies ($^{\circ}\text{C}$).

RSM produced a large difference in soil moisture ($+0.25 \text{ m}^3/\text{m}^3$) in all irrigated areas in January (Table 2), a result of specifying soil moisture at saturation

throughout the year. RSM also produced increased January T_{\min} values of 1°C to 4°C in the Central Valley, an effect that is not replicated in the other models (not

Table 2

Change in near-surface climate variables between NAT and MOD cases (MOD – NAT), spatially averaged over all grid cells specified as irrigated agriculture in MOD, with standard errors given in parentheses ($n=133$ for RSM, $n=65$ for RegCM3, $n=46$ for MM5-CLM3, and $n=64$ grid cells for DRCM)

Variable ^a	January				August			
	RSM	RegCM3	MM5-CLM3	DRCM	RSM	RegCM3	MM5-CLM3	DRCM
T_{mean}	0.23 (0.03)	0.06 (0.05)	-0.1 (0.1)	-0.11 (0.03)	-1.5 (0.1)	-3.1 (0.2)	-0.92 (0.07)	-1.4 (0.1)
T_{max}	-0.28 (0.05)	-0.15 (0.09)	-0.10 (0.08)	-0.27 (0.07)	-3.1 (0.3)	-6.1 (0.3)	-0.41 (0.03)	-2.9 (0.2)
T_{min}	0.76 (0.06)	0.22 (0.03)	0.0 (0.2)	0.05 (0.02)	1.99 (0.06)	-0.84 (0.09)	-1.4 (0.1)	0.10 (0.06)
DTR	-1.0 (0.1)	-0.37 (0.08)	-0.1 (0.1)	-0.32 (0.07)	-5.1 (0.3)	-5.3 (0.3)	0.9 (0.1)	-3.0 (0.2)
LHFS	1 (2)	2 (2)	-4.1 (0.7)	6 (1)	110 (3)	134 (3)	-0.6 (0.3)	100 (5)
SHFS	0 (1)	-1 (1)	4 (10)	-3.1 (0.8)	-102 (3)	-99 (3)	-20 (2)	-76 (4)
SMT	0.25 (0.009)	0.02 (0.006)	0.00 (0.004)	0.05 (0.008)	0.47 (0.003)	0.22 (0.004)	0.00 (0.000)	0.18 (0.006)
RHS	1.6 (0.6)	0.3 (0.5)	-2.4 (0.2)	1.9 (0.3)	35.8 (0.8)	23.0 (0.8)	1.6 (0.2)	8.8 (0.6)

^a T_{mean} , mean 2-m temperature ($^{\circ}\text{C}$); T_{max} , maximum 2-m temperature ($^{\circ}\text{C}$); T_{min} , minimum 2-m temperature ($^{\circ}\text{C}$); DTR, 2-m diurnal temperature range ($^{\circ}\text{C}$); LHFS, latent heat flux at land surface (W/m^2); SHFS, sensible heat flux at land surface (W/m^2); SMT, top soil layer soil moisture (m^3/m^3); RHS, 2-m relative humidity (%).

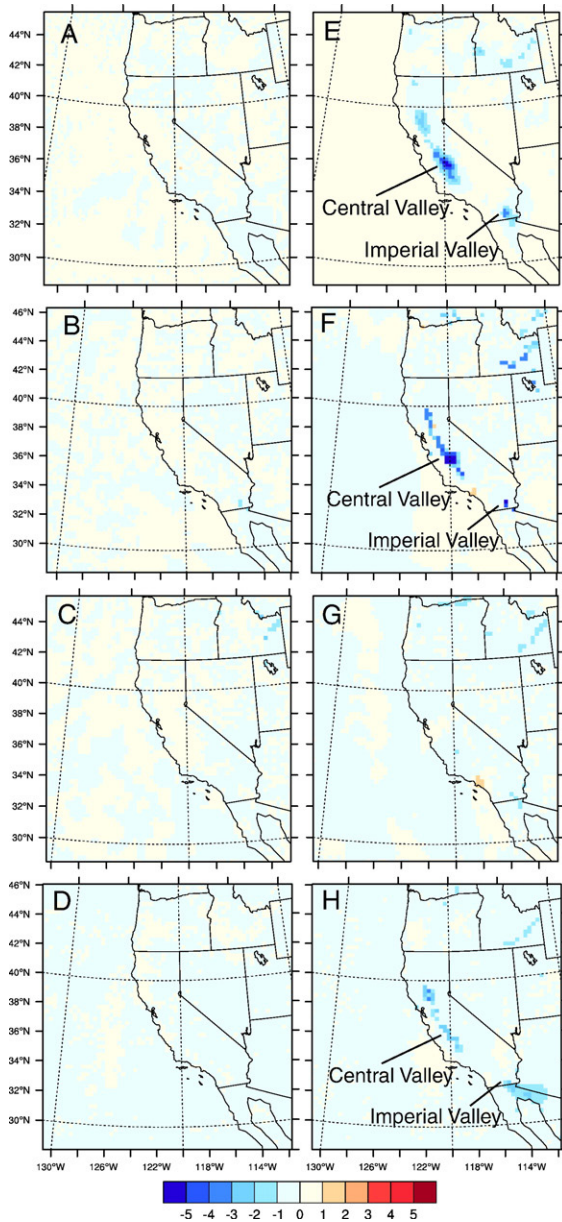


Fig. 5. January (left column) and August (right column) mean 2-m temperature (T_{mean}) anomalies (MOD – NAT) ($^{\circ}\text{C}$): (A) January RSM; (B) January RegCM3; (C) January MM5-CLM3; (D) January DRCM; (E) August RSM; (F) August RegCM3; (G) August MM5-CLM3; (H) August DRCM. Based on 57-year, 10-km reanalysis output generated by RSM (which does not include land use), the January T_{mean} standard deviation is 1.7 $^{\circ}\text{C}$ and the August T_{mean} standard deviation is 1.3 $^{\circ}\text{C}$, averaged over irrigated areas in this region (Kanamitsu and Kanamaru, in press).

shown). One area that experienced minor increases in January soil moisture and latent heat flux with irrigation in all three models was the otherwise warm, dry Imperial Valley (not shown).

4.3. Effects of converting natural vegetation to urban land-cover

The temperature effects of converting natural vegetation to urban land-cover were smaller and more diverse than the effects of conversion to irrigated agriculture, due to the smaller spatial extent of urban areas and considerable variation in urban parameterizations among the models (see Section 3.2 and Table 1). August T_{mean} and T_{min} increased with conversion to urban cover in all models but DRCM, which produced slight decreases (Table 3). T_{max} also increased in RSM, RegCM3, and DRCM, while decreasing in MM5-CLM3 (Table 3). As a result of the diverse changes in T_{max} and T_{min} , diurnal temperature range increased in RSM and DRCM, was unchanged in RegCM3, and decreased in MM5-CLM3 (Table 3). Soil moisture increased, latent heat flux decreased, and sensible heat flux increased in RSM and RegCM3 (Table 3) reflecting combined changes in vegetation cover, stomatal resistance, and soil properties (Table 1). Soil moisture was kept low in DRCM (Table 1), which also produced decreased latent and increased sensible heat fluxes. MM5-CLM3 represented urban land as bare ground, and as a result produced decreased soil

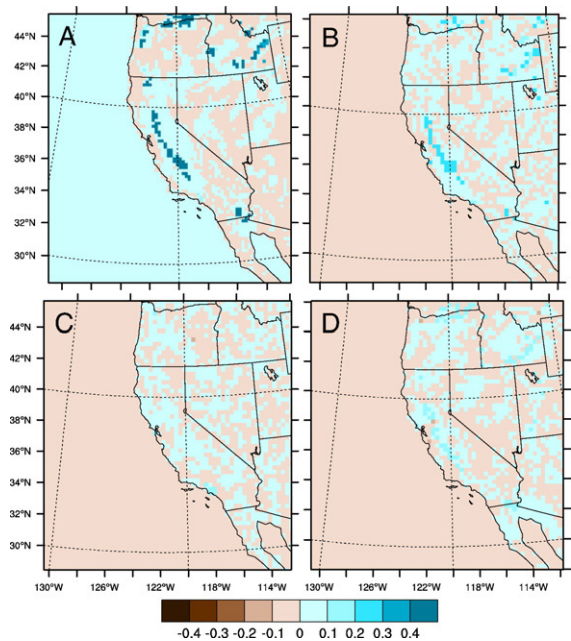


Fig. 6. August soil moisture anomalies (MOD – NAT) in m^3/m^3 : (A) RSM; (B) RegCM3; (C) MM5-CLM3; (D) DRCM. Based on 57-year, 10-km reanalysis output generated by RSM (which does not include land use), the August soil moisture standard deviation is 0.009 m^3/m^3 , averaged over irrigated areas in this region (Kanamitsu and Kanamaru, in press).

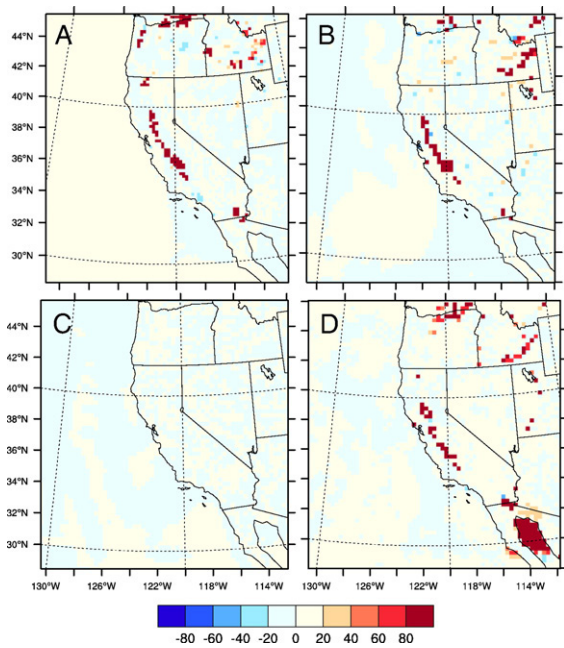


Fig. 7. August latent heat flux anomalies (MOD – NAT) in W/m^2 : (A) RSM; (B) RegCM3; (C) MM5-CLM3; (D) DRCM. Based on 57-year, 10-km reanalysis output generated by RSM (which does not include land use), the August latent heat flux standard deviation is $15.8 W/m^2$, averaged over irrigated areas in this region (Kanamitsu and Kanamaru, in press).

moisture, decreased latent and increased sensible fluxes (Table 3).

In January, RSM and RegCM3 produced changes in temperatures, energy fluxes and humidity of the same

sign as those in August, but DRCM and MM5-CLM3 produced more idiosyncratic results (Table 3). Unlike with conversion to irrigated agriculture, conversion of natural vegetation to urban land resulted in similarly small temperature effects ($\leq 1^\circ C$) in January and August (with the exception of MM5-CLM3 increases in T_{min} of $2.0^\circ C$) (Table 3). By way of comparison, January T_{mean} and August T_{mean} standard deviations were $1.9^\circ C$ and $1.2^\circ C$, respectively, in 57-year, 10-km reanalysis output generated by RSM (which does not include land-use) averaged over all urban areas in the domain (Kanamitsu and Kanamaru, in press).

5. Discussion

5.1. Latent cooling dominates temperature effects of irrigation

In the three models that supplemented soil moisture to higher levels under irrigated agriculture (RSM, RegCM3, and DRCM), changes in surface air temperature largely consistent with theoretical predictions were found. That is, by significantly increasing water available for evaporation, without substantially altering energy absorbed at the surface, under otherwise dry conditions there should be an increase in latent energy flux (Bonan, 2002). Converting natural vegetation to irrigated crops did in fact lead to a shift from sensible to latent heat flux, which in turn resulted in lower mean and maximum surface air temperatures during the dry season. It also resulted in substantially

Table 3

Change in near-surface climate variables between potential NAT and MOD cases (MOD – NAT), spatially averaged over all grid cells specified as urban in MOD, with standard errors given in parentheses ($n=18$ for RSM, $n=11$ for RegCM3, $n=11$ for MM5-CLM3, and $n=11$ for DRCM)

Variable ^a	January				August			
	RSM	RegCM3	MM5-CLM3	DRCM	RSM	RegCM3	MM5-CLM3	DRCM
T_{mean}	0.16 (0.07)	0.51 (0.09)	-0.39 (0.05)	0.10 (0.05)	0.29 (0.08)	1.1 (0.2)	0.8 (0.1)	-0.3 (0.2)
T_{max}	0.21 (0.06)	0.67 (0.08)	-0.50 (0.08)	0.29 (0.06)	0.6 (0.3)	1.0 (0.3)	-0.4 (0.1)	0.1 (0.2)
T_{min}	0.16 (0.04)	0.5 (0.1)	-0.1 (0.2)	-0.19 (0.05)	0.3 (0.1)	1.0 (0.1)	2.0 (0.2)	-0.5 (0.2)
DTR	0.05 (0.06)	0.2 (0.2)	-0.4 (0.2)	0.48 (0.09)	0.3 (0.3)	0.0 (0.4)	-2.4 (0.3)	0.6 (0.3)
LHFS	-4 (2)	-5 (1)	-2.8 (0.9)	-9 (1)	-18 (2)	-15 (7)	-2.9 (0.8)	-9 (3)
SHFS	4 (1)	10 (1)	-5 (2)	9 (2)	17 (4)	17 (6)	-46 (4)	25 (4)
SMT	0.03 (0.01)	0.21 (0.04)	0.03 (0.01)	-0.14 (0.02)	0.04 (0.01)	0.14 (0.03)	0.12 (0.01)	-0.07 (0.02)
RHS	-1.1 (0.3)	-2.8 (0.4)	0.9 (0.4)	-1.3 (0.3)	-0.1 (0.8)	-3.1 (0.9)	-0.6 (0.4)	1.1 (0.4)

^a Variables and units as in Table 2.

higher relative humidity. As demonstrated by the MM5-CLM3 results, conversion of natural vegetation to non-irrigated agriculture does not appear to have a strong influence on 2-m air temperatures in this region.

In the three models that included irrigation, the largest temperature effects were found during the summer (dry) months of July and August, with some differences beginning as early as March. The largest decreases in T_{mean} occurred over California's Central and Imperial Valleys. T_{max} dropped even more than T_{mean} , by -6.1 °C in RSM, -8.2 °C in RegCM3, and -4.7 °C in DRCM in August in the Central Valley. These temperature changes are consistent with a 20-year study using RegCM3 in California, which found statistically significant drops of 3.7 °C in August mean, and 7.5 °C in August maximum temperatures in areas converted to irrigated agriculture (Kueppers et al., 2007). July maximum temperatures under three different irrigation schemes (soil moisture supplemented to saturation, field capacity and wilting point) in this region also consistently decreased proportional to soil moisture in RSM (Kanamaru and Kanamitsu, unpublished manuscript). When irrigation was added to MM5-CLM3, this model also achieved a cooling effect, with the size of the cooling directly related to the degree of soil moisture enhancement (Jin and Miller, submitted for publication-b). Interestingly, RegCM3 produced a larger average effect on the mean and maximum 2-m air temperatures between June and September than did RSM, even though RSM forced the soil moisture content to a higher level (saturation, all soil pore space is filled with water) than RegCM3 (field capacity, soil pore space is partially filled with water). This was also in spite of the fact that sensible heat flux decreases were very similar between RSM and RegCM3, although the latent heat flux increased slightly more in RegCM3. Thus, the sign of the irrigation effect on mean and maximum temperatures was largely consistent across models, but the magnitude of the effect varies according to differences in how the models altered soil moisture content, as well as to differences in atmospheric dynamics and radiative transfer, soil texture, soil thermal diffusion, and albedo.

The models produced diverse results for the sensitivity of T_{min} to the conversion to irrigated agriculture. RSM produced an increase in August T_{min} of up to 2 °C, while RegCM3 produced a decrease of 1 °C averaged over all irrigated areas, and DRCM produced near zero change. The warming effect in RSM was most pronounced in the Central Valley, and persisted regardless of whether soil moisture was supplemented to satura-

tion, field capacity or the wilting point (Kanamaru and Kanamitsu, unpublished manuscript). Conversely, over a 20-year time period, RegCM3 found little consistent effect of irrigation on T_{min} (Kueppers et al., 2007). When irrigation was added to MM5-CLM3, T_{min} increased or decreased, depending on irrigation intensity (Jin and Miller, submitted for publication-b). In this study, nighttime sensible heat flux was negative (net heat uptake by the ground surface) in the NAT case for both RSM and RegCM3, indicating that the ground was colder than the air. Under irrigation, nighttime sensible heat flux was even more negative in RegCM3, perhaps because the daytime sensible heating was reduced due to the increase in moisture availability and the increase in latent heat flux. In RSM, the nighttime latent heat flux was negative, indicating that warming minimum temperatures could have been influenced by condensation and the release of latent heat to the lower atmosphere. The additional water vapor in the MOD case should result in a higher dew-point temperature, limiting nighttime cooling. Less daytime heating of the soil surface and higher dew-point temperatures with higher humidity should occur in all models. Differences in soil properties and natural vegetation types among the models may also help explain the differences in response via their effects on soil heat capacity and conductivity, and on the nighttime soil–air temperature gradient. In RSM, processes leading to T_{min} warming apparently won out, while they canceled or led to a slight T_{min} cooling in DRCM and RegCM3, respectively.

Christy et al. (2006) presented an analysis of observations in the southern portion of the California Central Valley (San Joaquin Valley) showing that during the twentieth century, there have been fairly large, and seasonally consistent, increases in T_{min} and only small decreases in T_{max} in the summer months. Christy et al. interpret these temperature changes to the expansion of irrigated areas over time. However, the present model simulations produce relatively small changes in T_{min} and large decreases in T_{max} when natural vegetation is converted to irrigated agriculture in a sensitivity study. There are at least three factors that may help to explain this disparity. First, no warming due to enhanced greenhouse gas (GHG) concentrations was included in these model simulations, but GHG effects would have influenced the observational records. Greater GHG concentrations would have dampened the decreases in T_{max} produced by the models, enhanced any warming in T_{min} , and dampened or reversed cooling of T_{min} in the models. Second, radiative effects of aerosols were not included in the model simulations. Buildup of aerosols near the surface from farm activities, vehicle

emissions, and industrial sources have increased the trapping of outgoing infrared radiation (IR) at night and raised T_{\min} in the observed temperature time series, but not in the models. Finally, the models may differ in their representation of the nighttime shallow boundary layer structure. A realistically shallow boundary layer would amplify any aerosol effect and possibly increase near surface humidity and stability, leading to less nighttime IR loss. Lack of a realistic representation of this structure in the models would minimize this nighttime effect.

The modeled surface temperature response to the conversion of natural vegetation to irrigated agriculture reported here is consistent with other modeling studies in this and other semi-arid regions (e.g., Adegoke et al., 2003; Boucher et al., 2004; Lobell et al., 2006; Kueppers et al., 2007; Kanamaru and Kanamitsu, unpublished manuscript). However, unlike some other studies (Barnston and Schickedanz, 1984; Segal et al., 1998) this study found no discernible effects on precipitation (data not shown). This discrepancy may be explained by the fact that precipitation along the west coast of the United States is very much a winter season phenomenon, controlled by large-scale weather systems. The greatest land-use impacts are seen in summer, when precipitation rarely occurs in this region. A series of 7-day continental-scale integrations show precipitation changes in other irrigated regions within the United States, but no or negligible changes in the western-most states (Segal et al., 1998).

Although this study found no discernible difference in precipitation between cases, it did find that RSM and RegCM3 produced slight increases in surface pressure over irrigated areas, which led to small effects on surface winds. With the surface air temperature cooling in the MOD case, the surface pressure increased up to 0.6 hPa in RSM, and up to 1 hPa in RegCM3 in August. As a result, the low-level westerlies into the Central Valley weakened. There were few changes in pressure height and wind above 850 hPa. These surface pressure and wind changes were the only impacts on the local atmospheric dynamics due to the land-use changes, and these effects seem to be confined to the boundary layer. Although it would be difficult to detect at the current model resolution, the fact that many of the irrigated areas are in valleys suggests that changes to the surface energy and water budgets with irrigation could alter mountain/valley circulations, particularly in summer, when synoptic influences are minimal. The land-use changes did not affect cloudiness or incoming solar radiation at the surface in the current experiment.

5.2. Diverse temperature responses to urban land-cover change

Changing from a natural landscape to one with urban land-cover leads to small changes in temperature. Urban land-cover typically has a lower albedo than the natural land-cover it replaces (Sailor, 1995), increasing the amount of solar radiation absorbed by the land surface. This study found that in RegCM3 and RSM this increased absorption led to increased sensible heat flux at the surface. The increased sensible heat flux led to increased T_{\max} , T_{mean} , and T_{\min} . In August, DTR also increased because the increase in T_{\max} was greater than the increase in T_{\min} for both models. Sensible heat flux and 2-m temperature changes were less consistent in DRCM and MM5-CLM3 with the conversion to urban land-cover. Latent heat flux was decreased in all models due to the removal (MM5-CLM3) or decrease in the amount (RegCM3, DRCM) of vegetation in the urban land-cover type. Stomatal resistance was also increased in some models (RSM, RegCM3) reducing transpiration, and thus latent heat flux. Finally, RegCM3 had less permeable soil under urban land and DRCM limited the soil moisture levels, decreasing the availability of soil water for evaporation. The decrease in latent heat flux was largest in the summer months. In sum, in this western U.S. region, the temperature signal of changing land-cover from natural vegetation to urban land was dependent upon both the parameterization of the urban land-cover type and the natural vegetation type that was replaced, and was not always consistent across models.

6. Conclusions

Land-use change in the western United States has the potential to alter surface temperatures, humidity, and energy fluxes, particularly during the warm, dry summer months. Multiple models detected temperature responses to conversion of natural vegetation to irrigated agriculture and urban land in California and Idaho. The modeled effects of urbanization are generally less consistent across models, due to the diversity of model parameterizations implemented. The nature of these model parameterizations for both irrigated agriculture and urban land, and relevant physical processes need to be assessed more rigorously, and refined to more closely represent anthropogenic land surface processes. Comparison of model results with atmospheric profiles of moisture, temperature, winds, and other variables should be undertaken to understand whether irrigation and urbanization effects can be detected at higher altitudes in this region, as Boucher et al. (2004) have reported based on a global

simulation of irrigation. Ultimately, to verify model results and lend confidence in predictions for the climate effects of future land-use change, high-resolution and long-term observational datasets of surface meteorology and land-use are needed.

The model results described here demonstrate the effects of converting natural vegetation to both urban and irrigated agricultural land for a single year with average precipitation. Interactions between these two types of land-use change may have enhanced, dampened or masked independent effects. For example, the grid cell representing the urban area of Sacramento lies in California's Central Valley (Fig. 1). The strong cooling in adjacent cells converted to irrigated agriculture likely influenced the August temperature change through advection into the Sacramento grid cell (Fig. 5). The results also do not include the indirect effects of urban and agricultural land-use on temperature via atmospheric loading of aerosols from industrial, transportation, or soil sources. Work by Jacobson (2004) and Rosenfeld and Givati (2006) has found that past additions of aerosols to California's atmosphere may have reduced incoming solar radiation and altered precipitation patterns.

Finally, the models used fairly simple schemes to represent irrigation, probably overestimating the amount of latent cooling. Compared to the CRU observations, RegCM3, RSM and DRCM produced T_{mean} and T_{max} values that were too low in the Central Valley in August, indicating that the models may be over-estimating the amount of irrigation water in the soils in this area. Integrating available data on irrigation amounts and timing into future experiments will produce refined estimates. Urban land-cover parameterizations also differed widely among the models, resulting in diverse and sometimes inconsistent temperature impacts from conversion of natural vegetation to urban land. RCMs at a sufficiently high spatial resolution are needed to represent major urban areas well, and would benefit from an urban scheme designed to capture aggregate physical properties of urban areas, including anthropogenic heating, and their atmospheric influences.

Acknowledgements

This work was funded by the California Energy Commission Public Interest Energy Research (PIER) program, which supports the California Climate Change Center. RegCM3 computations were carried out at the UCSC Climate Change and Impacts Laboratory, funded in part by NSF-ATM0215934. The authors thank G. Franco for helpful conversations and comments on earlier

versions of the manuscript, and anonymous reviewers for suggestions that significantly improved the paper. Thanks to S. Bryant (UCSC) for assistance with model runs, urban parameterizations, and data analysis, and T. O'Brien (UCSC) for assistance with figure preparation.

References

- Adegoke, J.O., Pielke, R.A.S., Eastman, J.L., Mahmood, R., Hubbard, K.G., 2003. Impact of irrigation on midsummer surface fluxes and temperature under dry synoptic conditions: a regional atmospheric model study of the U.S. High Plains. *Monthly Weather Review* 131, 556–564.
- Anderson, B.T., Roads, J.O., Chen, S.C., Juang, H.M.H., 2000. Regional simulation of the low-level monsoon winds over the Gulf of California and southwestern United States. *Journal of Geophysical Research – Atmospheres* 105 (D14), 17955–17969.
- Arnfeld, A.J., 2003. Two decades of urban climate research: a review of turbulence, exchanges of energy and water, and the urban heat island. *International Journal of Climatology* 23, 1–26.
- Barnston, A.G., Schickedanz, P.T., 1984. The effect of irrigation on warm season precipitation in the southern Great Plains. *Journal of Climate and Applied Meteorology* 23 (6), 865–888.
- Bell, J.L., Sloan, L.C., Snyder, M.A., 2004. Regional changes in extreme climatic events: a future climate scenario. *Journal of Climate* 17, 81–87.
- Bonan, G., 2002. *Ecological Climatology*. Cambridge University Press, Cambridge. 678 pp.
- Boucher, O., Myhre, G., Myhre, A., 2004. Direct human influence of irrigation on atmospheric water vapor and climate. *Climate Dynamics* 22, 597–603.
- Chen, F., Dudhia, J., 2001. Coupling an advanced land surface–hydrology model with the Penn State–NCAR MM5 modeling system: Part I. Modeling implementation and sensitivity. *Monthly Weather Review* 129, 569–585.
- Chen, S.C., Roads, J.O., Juang, H.M.H., Kanamitsu, M., 1999. Global to regional simulations of California wintertime precipitation. *Journal of Geophysical Research – Atmospheres* 104 (D24), 31517–31532.
- Chou, M.-D., Lee, K.-T., 1996. Parameterizations for the absorption of solar radiation by water vapor and ozone. *Journal of Atmospheric Science* 53, 1203–1208.
- Chou, M.-D., Suarez, M.J., 1994. An Efficient Thermal Infrared Radiation Parameterization for Use in General Circulation Models. TM-1994-104606, 3. National Aeronautical and Space Administration.
- Christy, J.R., Norris, W.B., Redmond, K., Gallo, K.P., 2006. Methodology and results of calculating central California surface temperature trends: evidence of human-induced climate change? *Journal of Climate* 19 (4), 548–563.
- Dickinson, R.E., Henderson-Sellers, A., Kennedy, P.J., 1993. Biosphere–Atmosphere Transfer Scheme (BATS) Version 1e as Coupled to the NCAR Community Climate Model. NCAR TN-387+STR. NCAR, Boulder, CO.
- Eliasson, I., Svensson, M.K., 2003. Spatial air temperature variations and urban land use – a statistical approach. *Meteorological Applications* 10, 135–149.
- Elvidge, C.D., et al., 2004. U.S. constructed area approaches the size of Ohio. *EOS, Transactions, American Geophysical Union* 85 (24), 233.
- Feddema, J.J., et al., 2005. The importance of land-cover change in simulating future climates. *Science* 310, 1674–1678.

- Fritsch, J.M., Chappell, C.F., 1980. Numerical prediction of convective driven mesoscale pressure systems: 1. Convective parameterization. *Journal of the Atmospheric Sciences* 37 (8), 1722–1733.
- Gibson, J.K., et al., 1997. ERA Description. ECMWF Re-Analysis Final Report Series. 71 pp.
- Giorgi, F., Hurrell, J.W., Marinucci, M.R., Beniston, M., 1997. Elevation dependency of the surface climate change signal: a model study. *Journal of Climate* 10, 288–296.
- Grell, G.A., 1993. Prognostic evaluation of assumptions used by cumulus parameterizations. *Monthly Weather Review* 121 (3), 764–787.
- Holtlag, A.A.M., Boville, B.A., 1993. Local versus nonlocal boundary-layer diffusion in a global climate model. *Journal of Climate* 6 (10), 1825–1842.
- Hong, S.-Y., Pan, H.L., 1996. Nonlocal boundary layer vertical diffusion in a medium-range forecast model. *Monthly Weather Review* 124, 2322–2339.
- Jacobson, M.Z., 1999. Effects of soil moisture on temperatures, winds, and pollutant concentrations in Los Angeles. *Journal of Applied Meteorology* 38, 607–616.
- Jacobson, M.Z., 2004. Effects of Anthropogenic Aerosol Particles and their Precursor Gases on California and South Coast Climate Final Report to the California Energy Commission.
- Janjic, Z.I., 1990. The step-mountain coordinate: physical package. *Monthly Weather Review* 118, 1429–1443.
- Janjic, Z.I., 1994. The step-mountain Eta coordinate model – further developments of the convection, viscous sublayer, and turbulence closure schemes. *Monthly Weather Review* 122, 927–945.
- Jin, J., and Miller, N.L., submitted for publication-a. Coupling of an advanced land surface model with MM5 to improve regional snow simulations. *Journal of Geophysical Research*.
- Jin, J. and Miller, N.L., submitted for publication-b. Regional climate simulations to quantify the range of land use change and irrigation impacts on the hydroclimate in the California Central Valley. *Journal of Geophysical Research*.
- Jin, M., Dickinson, R.E., Zhang, D.-L., 2005. The footprint of urban areas on global climate as characterized by MODIS. *Journal of Climate* 18, 1551–1565.
- Juang, H.-M., Kanamitsu, M., 1994. The NMC nested regional spectral model. *Monthly Weather Review* 122, 3–26.
- Kanamaru, H., Kanamitsu, M., 2005. Scale Selective Bias Correction in Downscaling of Global Analysis Using a Regional Model. CEC-500-2005-130. California Energy Commission, Sacramento.
- Kanamitsu, M., and Kanamaru, H., in press. 57-year California reanalysis downscaling at 10 km (CaRD10): Part 1. System detail and validation with observations. *Journal of Climate*.
- Kanamitsu, M., et al., 2002. NCEP-DOE AMIP-II Reanalysis (R-2). *Bulletin of the American Meteorological Society* 83 (11), 1631–1643.
- Kanamitsu, M., Kanamaru, H., Cui, Y., Juang, H., 2005. Parallel Implementation of the Regional Spectral Atmospheric Model. CEC-500-2005-014. California Energy Commission, Sacramento.
- Kiehl, J.T., Hack, J.J., Briegleb, B.P., 1994. The simulated earth radiation budget of the NCAR CCM2 and comparison with the earth radiation budget experiment. *Journal of Geophysical Research* 99, 20815–20827.
- Kiehl, J.T., et al., 1996. Description of the NCAR Community Climate Model (CCM3). NCAR TN-420+STR, CGD, NCAR.
- Kim, J., 2001. A nested modeling study of elevation-dependent climate change signals in California induced by increased atmospheric CO₂. *Geophysical Research Letters* 28 (15), 2951–2954.
- Kim, J., Kim, T.K., Arritt, R., Miller, N.L., 2002. Impacts of increased atmospheric CO₂ on the hydroclimate of the western United States. *Journal of Climate* 15, 1926–1942.
- Kueppers, L.M., Snyder, M.A., Sloan, L.C., 2007. Irrigation cooling effect: regional climate forcing by land use change. *Geophysical Research Letters* 34, L03703. doi:10.1029/2006GL028679.
- Lal, R., Bruce, J.P., 1999. The potential of world cropland soils to sequester C and mitigate the greenhouse effect. *Environmental Science and Policy* 2, 177–185.
- Leff, B., Ramankutty, N., Foley, J.A., 2004. Geographic distribution of major crops across the world. *Global Biogeochemical Cycles* 18, GB1009. doi:10.1029/2003GB002108.
- Leung, L.R., et al., 2004. Mid-century ensemble regional climate change scenarios for the western United States. *Climatic Change* 62, 75–113.
- Lin, Y.-L., Farley, R.D., Orville, H.D., 1983. Bulk parameterization of the snow field in a cloud model. *Journal of Climate and Applied Meteorology* 22, 1065–1092.
- Lobell, D.B., Bala, G., Duffy, P.B., 2006. Biogeophysical impacts of cropland management changes on climate. *Geophysical Research Letters* 33, L06708.
- Loveland, T.R., et al., 1995. Seasonal land-cover regions of the United States. *Annals of the Association of American Geographers* 85, 339–355.
- Loveland, T.R., et al., 2000. Development of a global land cover characteristics database and IGBP DISCover from 1-km AVHRR data. *International Journal of Remote Sensing* 21 (6/7), 1303–1330.
- Mitchell, T.D., Jones, P.D., 2005. An improved method of constructing a database of monthly climate observations and associated high-resolution grids. *International Journal of Climatology* 25, 693–712.
- Mlawer, E.J., Taubman, S.J., Brown, P.D., Iacono, R.J., Clough, S.A., 1997. Radiative transfer for inhomogeneous atmospheres: RRTM, a validated correlated-k model for the longwave. *Journal of Geophysical Research* 102, 16,663–16,682.
- Moorthi, S., Suarez, M.J., 1992. Relaxed Arakawa–Schubert: a parameterization of moist convection for general circulation models. *Monthly Weather Review* 120, 978–1002.
- Oke, T.R., 1981. Canyon geometry and the nocturnal urban heat island: comparison of scale model and field observations. *Journal of Climatology* 1, 237–254.
- Oleson, K.W., et al., 2004. Technical Description of the Community Land Model (CLM). NCAR/TN-461+STR.
- Pal, J.S., Giorgi, F., Bi, X., Elguindi, N., Solmon, F., Gao, X., Rauscher, S.A., Francisco, R., Zakey, A., Winter, J., Ashfaq, M., Syed, F., Bell, J.L., Diffenbaugh, N.S., Karmacharya, J., Konare, A., Martinez, D., Da Rocha, R.P., Sloan, L.C., Steiner, A., in press. Regional Climate Modeling for the Developing World: The ICTP RegCM3 and RegCM3. *Bulletin of the American Meteorological Society*.
- Pan, H.L., Mahrt, L., 1987. Interaction between soil hydrology and boundary-layer development. *Boundary-Layer Meteorology* 38 (1–2), 185–202.
- Pielke, R.A.S., et al., 2002. The influence of land-use change and landscape dynamics on the climate system: relevance to climate-change policy beyond the radiative effect of greenhouse gases. *Philosophical Transactions of the Royal Society of London. Series A: Mathematical and Physical Sciences* 360, 1705–1719.
- Population Reference Bureau, 2004. 2004 World Population Data Sheet.
- Ramankutty, N., Foley, J.A., 1999. Estimating historical changes in global land cover: croplands from 1700 to 1992. *Global Biogeochemical Cycles* 13 (4), 997–1027.
- Reynolds, R.W., Rayner, N.A., Smith, T.M., Stokes, D.C., Wang, W., 2002. An improved in situ and satellite SST analysis for climate. *Journal of Climate* 15 (13), 1609–1625.
- Rosenfeld, D., Givati, A., 2006. Evidence of orographic precipitation suppression by air pollution induced aerosols in the western USA. *Journal of Applied Meteorology and Climatology* 45, 893–911.

- Sailor, D.J., 1995. Simulated urban climate response to modifications in surface albedo and vegetative cover. *Journal of Applied Meteorology* 34, 1694–1704.
- Sala, O.E., et al., 2000. Global biodiversity scenarios for the year 2100. *Science* 287, 1770–1774.
- Segal, M., Pan, Z., Turner, R.W., Takle, E.S., 1998. On the potential impact of irrigated areas in North America on summer rainfall caused by large-scale systems. *Journal of Applied Meteorology* 37, 325–331.
- Snyder, M.A., Sloan, L.C., 2005. Transient future climate over the Western U.S. using a regional climate model. *Earth Interactions* 9 (Paper 11).
- Snyder, M.A., Bell, J.L., Sloan, L.C., Duffy, P.B., Govindasamy, B., 2002. Climate responses to a doubling of atmospheric carbon dioxide for a climatically vulnerable region. *Geophysical Research Letters* 29 (11). doi:10.1029/2001GL014431.
- Tao, W.K., Simpson, J., McCumber, M., 1989. An ice-water saturation adjustment. *Monthly Weather Review* 117, 231–235.
- USDA, 2004. 2002 Census of Agriculture. USDA National Agricultural Statistics Service.
- Watson, R.T., et al. (Ed.), 2000. *Land Use, Land-Use Change, and Forestry*. Cambridge University Press, Cambridge. 377 pp.